FINITE ELEMENT SIMULATION OF INTERIOR BALLISTIC PROCESSES IN 120-mm MORTAR SYSTEM*

Ragini Acharya[1] and Kenneth K. Kuo[1]

[1]*High Pressure Combustion Laboratory, The Pennsylvania State University, University Park, PA 16802 USA email: rza101@psu.edu, kenkuo@psu.edu*

The objective of this work is theoretical modeling and numerical simulation of early-phase interior ballistic processes in various parts of 120-mm mortar system by developing a 3-D mortar interior ballistic (3DMIB) code. Due to the complexity of the overall interior ballistic processes in the mortar propulsion system, it is advantageous to solve the problem in a modular fashion, i.e., simulating each component of this propulsion system separately and interfacing these modules with appropriate boundary conditions. For the tail-boom section, method of characteristics (MOC) code was developed and validated by experimental test results. For combustion processes inside the tail-boom section are compared, using two different types of pyrotechnic materials (Black powder and MRBPS) in the flash tube. The combustion event starts earlier with MRBPS pellets and shows more rapid pressurization rate. In both cases, pressure traces showed significant axial pressure wave phenomena, which were simulated reasonably close to the measured pressure-time traces. The predicted pressure in the igniter end matched very well with the experimental data that was obtained later, thus affirming the reliability of the numerical code. For the mortar tube section, the finite element method (FEM) was utilized to develop a numerical code and the calculated results are partially validated by available experimental data. For the mortar tube section, the calculated results also exhibit similar pressure wave phenomena, observed in an instrumented high-pressure combustor simulator (IHPCS) with stationary projectile and controlled peak pressure.

INTRODUCTION

Simulation of the flame spreading and combustion processes in various parts of a 120-mm mortar system under realistic firing conditions is important for design modification to improve the system performance. The motivation for this work came through US Army's mortar firing experiments, in which some short rounds were

* Work sponsored by the US Army through the SAVIT Corporation. The support of Mr. Randy Rand and Mr. Jason Travaille of ARDEC and Mr. Jack Sacco of SAVIT is highly appreciated.

observed during test firings with damaged fin blades. These instances were attributed to fin blade damage during firing and provided the motivation for detailed modeling and stepwise experimental validation of the model predictions of the combustion behavior of the ignition cartridge and propelling charge increments in the mortar system. The motivation of this work is to gain deeper understanding of the interior ballistic processes from detailed simulation of various parts of the mortar propulsion system. This study can also help to advance future improvements of the propulsion unit to achieve greater reliability in mortar performance. The specific objectives of this work are: (i) to compare the interior ballistic processes in the granular bed of M1020 ignition cartridge of the 120-mm mortar system using Black Powder (BP) and Moisture Resistant Black Powder Substitute (MRBPS) as two different pyrotechnic materials, (ii) to simulate the interior ballistic processes in the mortar tube with propelling charges increments loaded on the tail-boom section. The comparison of two pyrotechnic materials also facilitates model validation with more than one type of pellets in the flash tube, thus increasing the reliability of the numerical code. In modeling and simulation, the 120-mm mortar system was divided into three major parts; flash tube, tail boom, and mortar tube. The mortar interior ballistic (MIB) model and code has been developed with the stepwise validation by considering interior ballistic processes in a modular fashion under limiting conditions: a) ignition cartridge with no propellant charge increments loaded on its external surfaces, b) combustion processes of M234 propelling charges in the mortar tube, while the projectile body is held stationary, c) combustion processes of M234 propelling charges in the mortar tube, while the projectile body is moving. This paper addresses the computed results for cases (a) and (b).

IGNITION CARTRIDGE COMBUSTION SUBMODEL & COMPUTED RESULTS

A transient one-dimensional numerical code using method of characteristics was developed and validated by Kuo et al. [1] to simulate the interior ballistic processes of ignition cartridge without charge increments (i.e., case (a)), by discharging combustion products directly into the atmosphere. To simulate the combustion processes in the granular propellant bed loaded with M48 ball propellants, six coupled quasi-linear inhomogeneous hyperbolic partial differential equations (PDEs) were formulated by applying the principles of conservation of mass, momentum and energy for condensed phase and gas phase in the granular propellant bed. In order to solve these equations for quantities of interest [i.e. pressure, propellant-surface temperature, gas temperature, porosity (or called void fraction), gas velocity, and propellant particle velocity], they were converted to a system of ordinary differential equations (ODEs) using the method of characteristics (MOC).

A schematic drawing of the longitudinal cross-sectional view of the M1020 ignition cartridge is shown in Fig.1. In this design, the flash tube is initially loaded with five center-perforated cylindrical pyrotechnic pellets to generate combustion products, which flow into its cavity region and are partially discharged into the granular bed through 20 vent holes along the surface of flash tube. These vent holes are distributed at 10 different axial locations with alternative orientations (at 90° angle). The vent holes are numbered from 1 to 20 with number 1 starting from the primer end. There are total 28 vent holes on the cylindrical surface of the tail-boom and combustion products (both in gas-phase and condensed-phase) are discharged from these vent holes into the mortar tube section. As shown in Figs. 2(a)-(b), the combustion event inside the flash tube differs significantly between the two types of pyrotechnic pellets, with multiple peaks of gas-phase mass flow rates for black powder and a single but significantly larger peak of gas-phase mass flow rates for MRBPS pellets, due to higher percentage of gas-phase products from MRBPS.

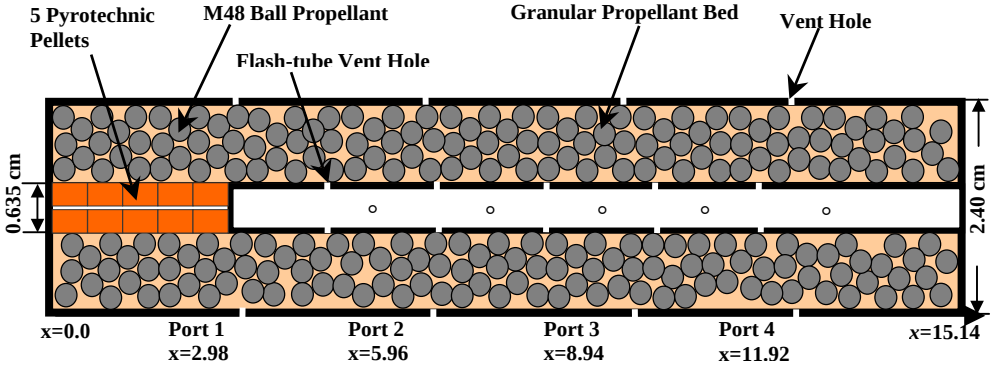

Figure 1. Schematic of Cross-Sectional View of the M1020 120-mm Ignition Cartridge of Mortar Projectile (*x* given in *cm*)

These gas-phase mass flow rates were deduced from the flash tube submodel and then used in the granular bed submodel for the determination of pressurization rates at various axial locations in the granular propellant bed. The calculated pressure-time traces are shown in Figures 3(a)-3(b), corresponding to BP and MRBPS pellets, respectively. In both figures, pressure at Port 4 location, P_4 starts to rise before Port 1 location. This behavior is attributed to stronger discharge of igniter products from the flash tube near P_4 location. The pressure rise starts earlier when MRBPS pellets are used in comparison with BP pellets due to earlier and higher rate of mass discharge. In general, the pressure wave behavior in the granular bed using MRBPS pellets in the initiator is similar to those using BP pellets as initiator. The computational results from the numerical code are compared with experimental results for the cases with BP pellets and MRBPS pellets shown in Figures 4(a)-4(b). The predicted pressure-time traces match the pressure wave phenomenon very closely for both BP and MRBPS cases as

well as the peak pressure magnitude and rise time. It is useful to note that the predicted maximum pressure occurred in the axial location (x = 0.48 *cm*) significantly below the P1 transducer location, which was not measured in the earlier set of experiments. After the numerical results were known, a pressure transducer port called P_0 was added to the tail-boom section. The recorded P_0-t traces were indeed much higher than the P_1-t traces as predicted by the computer code. This experimental confirmation further verifies the predictability of the numerical code.

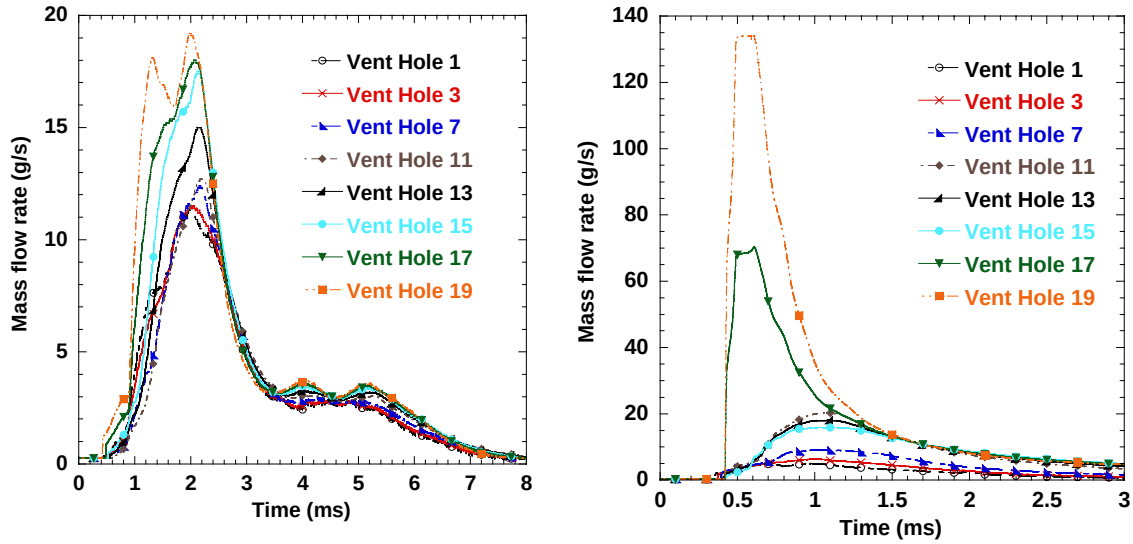

(a) Black Powder (BP) (b) MRBPS

Figure 2. Deduced mass flow rates of gas-phase products from flash tube

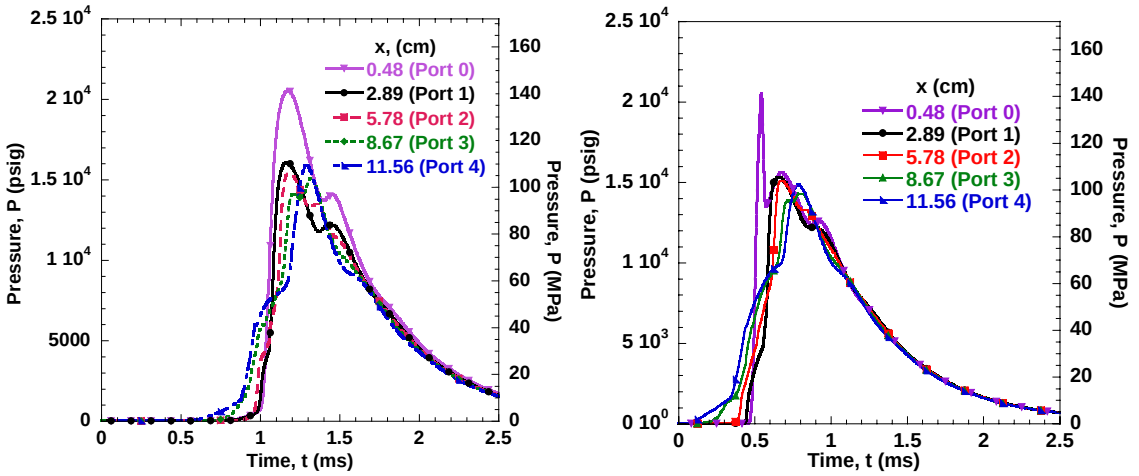

(a) Black Powder (BP) (b) MRBPS

Figure 3. Computed P-t traces in M1020 ignition cartridge using (a) Black powder pellets, and (b) MRBPS pellets in the flash tube

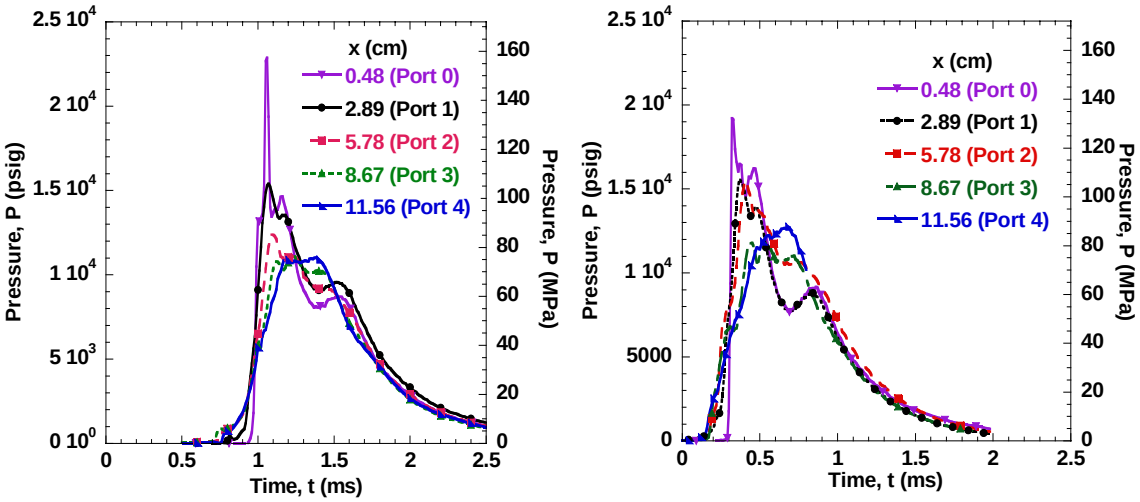

(a) Black Powder (BP) (b) MRBPS

Figure 4. Measured P-t traces in M1020 ignition cartridge using (a) Black powder pellets, and (b) MRBPS pellets in the flash tube from PSU test firing[†]

MORTAR TUBE COMBUSTION SUBMODEL & COMPUTED RESULTS

To simulate the ignition/combustion processes of the M47 granular propellants contained in M234 charge increments in the mortar tube, the transient gas dynamic behavior of hot product gas and particles from the vent holes of the tail-boom section are coupled with the heat-transfer, flame-spreading, combustion, and chamber pressurization process in the mortar tube. The energy equation for spherical particles in is solved to determine the onset of ignition of the propellant in the charge increments. The discharged mass and energy fluxes from a tail-boom vent hole are determined from the ignition cartridge submodel. In the mortar tube submodel, these data are used in the boundary conditions and as source terms in the governing equations. Due to the complex projectile geometry, a finite element method was used to solve the governing equations for the combustion processes. The mortar tube section is divided into a fin-blade region, a vent-hole region, a conical region and a projectile-payload region based upon the exact projectile geometry. The vent-hole region has 14 axial divisions, 5 radial divisions, and 5 angular divisions for a 1/8 portion of the full cross-section of the mortar projectile. Hence, there are a total of 350 elements in the 1/8 portion of the vent-hole region of mortar tube. The hexahedral finite element geometries are used for fin-blade region and vent-hole region. However, both the conical region and the projectile region have non-uniform areas; therefore a combination of hexahedral elements and wedge elements has been utilized for these regions. The computed mass fluxes of the

[†] The authors wish to acknowledge the assistance of Jeffrey D. Moore and Peter J. Ferrara of PSU.

combustion products per single tail-boom vent-hole area in the mortar tube section are shown in Figure 5. The non-uniform axial variation of the discharging combustion products from tail-boom causes the sequential pressurization event in the mortar tube. Since the uppermost vent-holes start discharging first, the propellant grains in the charge increment 4 are ignited earlier than other charge increments. These computed results correspond to a case of aligned horse-shoe shaped charge increments. Following the rapid combustion of M47 granular propellant grains in the charge increment 4, the pressure-waves are generated and they propagate in both directions toward fin-blade region and projectile-payload region. The pressurization processes in these two regions were the last to occur; the pressure in the fin-blade region rises faster than the other regions and later exceeds those at other regions. This phenomenon occurs due to the downward motion of propellant grains, which were driven by the pressure wave. The current computations end before the onset of projectile motion, which corresponds to case (b) as described earlier. In general, the calculated results at the fin-blade region (shown in Figure 6) are in the same peak pressure range and rise time of a measured pressure-time trace obtained from the base area of an actual mortar firing.

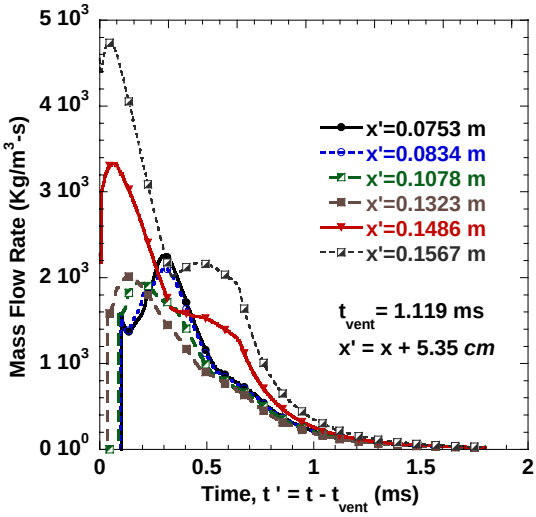

Figure 5. Computed local gaseous mass flow rate into charge increment section from tail-boom

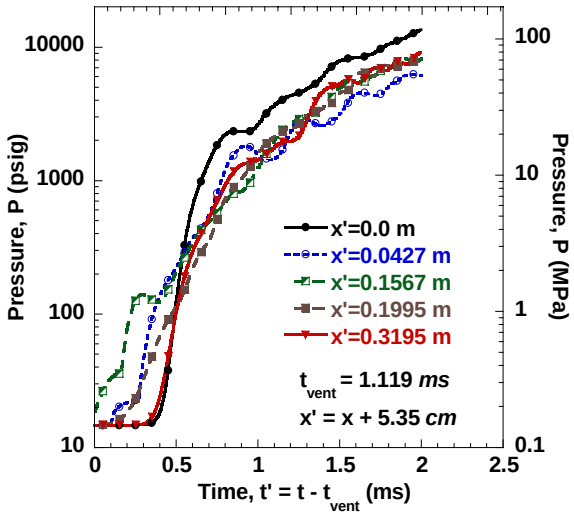

Figure 6. Computed P-t traces at various axial locations in the mortar tube

The early-phase pressure wave phenomena in the loaded portion of the mortar tube are further illustrated in the computed solution by the evolution of high-pressure zones from the vent-hole region toward both upward and downward directions in Figure 8. It can be clearly seen from these plots that the downward pressure wave is stronger toward the fin-blade region than the projectile-payload region in the upward direction. This is due to the vigorous burning of propellant grains from the charge increments that are located unevenly in the lower portion of the vent-hole region.

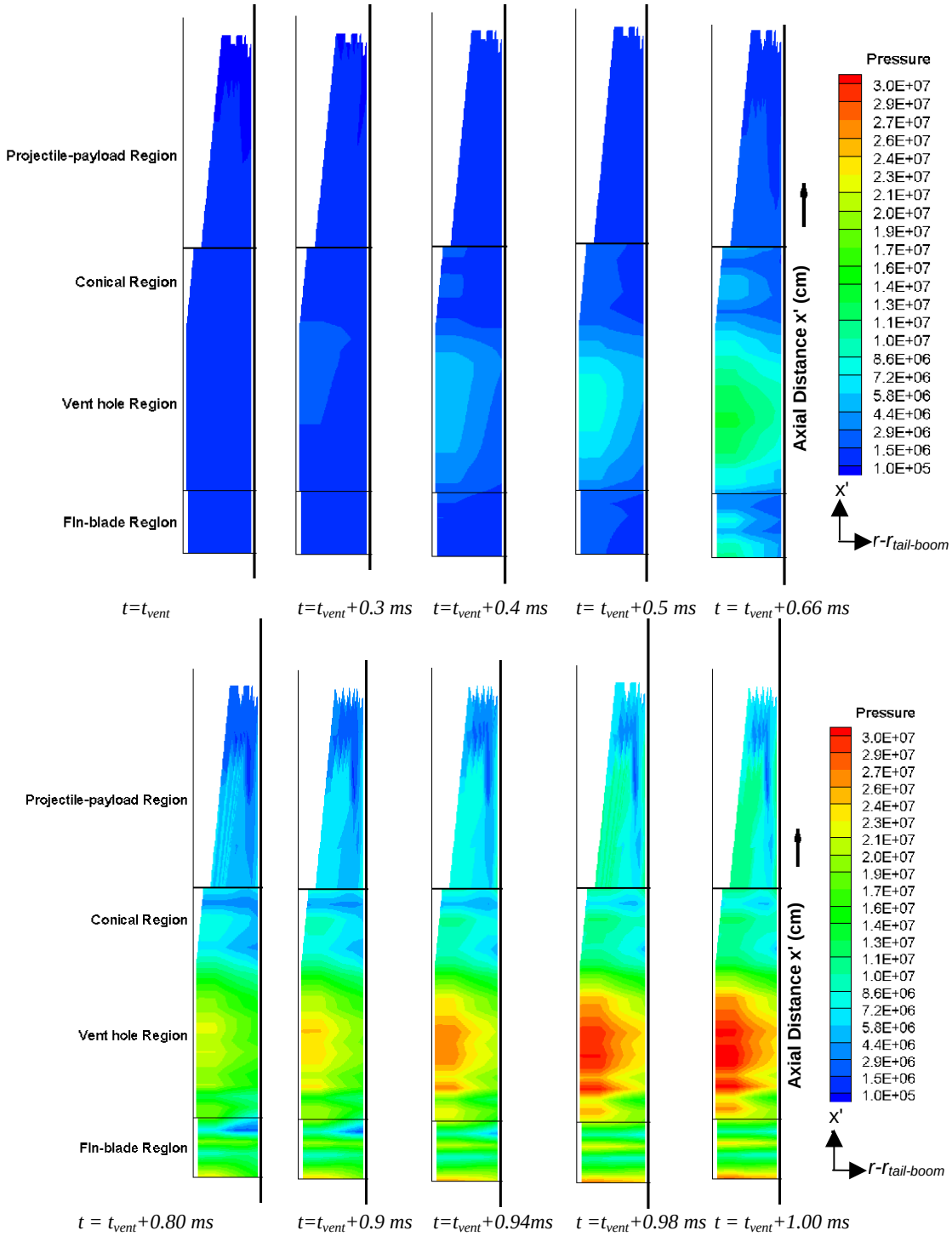

Figure 8. Computed early-phase pressure contours in the mortar tube at various times (*Pressure* in *Pa*)

The computed propellant surface temperature-time traces (calculated from code but not shown here) have confirmed that the propellant grains are ignited first in the upper portion of the vent-hole region (close to projectile-payload region) and then the flame spreads downward to other charge increments in the vent-hole region. This behavior is similar to that inside the tail-boom section due to early discharge of hot combustion products out of the vent holes at the uppermost axial location in the vent-hole region near the projectile end. The computed axial gas and particle velocity-time contours in the mortar tube (also not shown here due to limited space) indicate that the combustion products and burning granular propellant particles flow downward from vent-hole region to fin-blade region. Smaller portions of the gas and particle also flow upward into the conical and projectile-payload regions.

CONCLUSIONS

This work demonstrates the successful development of a 3D theoretical model and implementation of a numerical code for prediction of ignition/combustion, flame spreading, and pressurization processes in both the ignition cartridge and the mortar tube sections of the 120-mm mortar propulsion system before the onset of projectile motion. The computational results are partially validated by experimental data from both ignition cartridge and mortar tests. The computed results show the pressure wave generation, propagation, and wave-reflection in both ignition cartridge and mortar tube sections. The pressure wave in the ignition cartridge is mainly due to the uneven discharge of combustion products from the flash tube. The discharge of combustion products from the tail-boom vent-holes also occurs in the same sequence as the flash tube. The non-uniform burning in the ignition cartridge combined with the uneven loading of M47 propellant grains in the mortar tube can result in a strong pressure-wave generation in the mortar. The overall combustion process in the existing configuration is strongly influenced by the non-uniformity of mass and energy discharge from flash tube. It is expected that the 3DMIB model/numerical simulation work can provide useful guidance to the future design improvements of the mortar propulsion systems.

REFERENCES

[1] K. K. Kuo, R. Acharya, P. J. Ferrara, and J. D. Moore, “Method of Characteristics Simulation of Interior Ballistic Processes of M1020 Ignition Cartridge in a 120-mm Mortar System”, Accepted for publication in the *Advancements in Energetic Materials & Chemical Propulsion* to be published by Begell House Publisher, June 2006, Also presented at the *6-International Symposium on Special Topics in Chemical Propulsion*, Santiago, Chile, March 8-11, 2005.